Journal of Magnetic Resonance 196 (2009) 7–11

Contents lists available at ScienceDirect

Journal of Magnetic Resonance

journal homepage: www.elsevier.com/locate/jmr

Globally optimal superconducting magnets Part II: Symmetric MSE coil arrangement

Quang M. Tieng, Viktor Vegh *, Ian M. Brereton

Centre for Magnetic Resonance, The University of Queensland, Research Road, Brisbane, St. Lucia Q4072, Australia

ARTICLE INFO

Article history:
Received 30 June 2008
Revised 2 September 2008
Available online 30 September 2008

Keywords:
Superconducting magnet
Global optimization
Coil layout
Magnet design
Sequential quadratic programming

ABSTRACT

A globally optimal superconducting magnet coil design procedure based on the Minimum Stored Energy (MSE) current density map is outlined. The method has the ability to arrange coils in a manner that generates a strong and homogeneous axial magnetic field over a predefined region, and ensures the stray field external to the assembly and peak magnetic field at the wires are in acceptable ranges. The outlined strategy of allocating coils within a given domain suggests that coils should be placed around the perimeter of the domain with adjacent coils possessing alternating winding directions for optimum performance. The underlying current density maps from which the coils themselves are derived are unique, and optimized to possess minimal stored energy. Therefore, the method produces magnet designs with the lowest possible overall stored energy. Optimal coil layouts are provided for unshielded and shielded short bore symmetric superconducting magnets.

1. Introduction

Magnetic resonance technology has been a key diagnostic tool for many years and the technology continues to mature in applications within the clinical and research settings [1]. A number of advancements in design have seen the development of improved and cheaper technologies in magnet construction and performance [2–9], which provide clear benefits to the community in the form of more accurate and insightful diagnostic and preventative healthcare. Recent emerging technologies have provided practitioners with the ability to obtain higher resolution images, and perform faster scans, resulting in greater patient throughput and improved patient comfort.

The aim of this research work is to develop techniques of designing ultra-short bore superconducting magnets to be used in MRI and NMR experiments. It is envisaged that the magnets will be constructed using less superconducting material, and therefore incur lower manufacturing costs and ultimately translate to more affordable systems and lower future scan costs. An equally important benefit of shorter magnets is reduced patient claustrophobia experienced during examination. Due to a reduced magnet bore length, the more open magnet design should allow better patient access and enhance interventional MRI procedures, in conjunction with intra-operative scanning.

The current generation of MRI/NMR superconducting magnets emerged over a decade ago employing active shielding, in which negative current coils within the design are incorporated to generate magnetic fields that reduce the "stray" field outside the magnet structure generated by the positive current magnet coils. Attempts have been made to address the concerns of weight, size and magnetic field nonlinearity [2–4] in these magnet systems, with the hope of manufacturing less costly systems.

The primary requirement of an NMR/MRI superconducting magnet is to generate a strong and homogenous axial magnetic field over the imaging region, which is commonly referred to as the Diameter Spherical Volume (DSV) [10]. The magnet must be designed and built in such a way as to restrict the peak magnetic field produced inside the superconductors themselves, and minimize the existence of magnetic fields external to the assembly [11]. Minimization of the external fields is called shielding, and is usually performed by placing coils as part of the assembly on the exteriors of the magnet, to minimize the extent of the stray field. Usually, active shielding is a process whereby coils with reverse current directions are placed on the outer diameter of the main windings to reduce stray magnetic fields exterior to the magnet chamber.

Other factors that influence the design and manufacturing of magnets are related to geometrical constraints, including the length of the magnet and associated wire cost. The preceding publication, Part I [12], outlined the method of obtaining a minimum stored energy (MSE) current density map, and here we describe the design of a symmetrical magnet by appropriate placement of coils in locations determined from the MSE current density map.

The proposed MSE method of designing superconducting magnets consists of two specific steps:

* Corresponding author. Fax: +61 7 3365 3833.
E-mail address: v.vegh@uq.edu.au (V. Vegh).

1090-7807/$ - see front matter
doi:10.1016/j.jmr.2008.09.023

(a) Part I: To determine the MSE current density map over a predefined domain subject to constraints, such as the homogeneity of the DSV and the size of the magnet stray field. The optimal MSE current density map is found by changing the size of the magnet domain and by adjusting the number of internal and external harmonic coefficients to be eliminated.
(b) Part II: To determine the final magnet arrangement with the initial coil layout based on the current density map. The coil locations and sizes are refined to enhance the field homogeneity and to decrease the footprint of the magnet field, without changing the constraint definition for the MSE current density map.

2. Superconducting coil refinement

Given the magnet requirements and using the general technique outlined in [12], an MSE current density map is obtained. The MSE current density map obtained in this manner generally has several local maxima and minima within the magnet domain referred to as extremities. The number of extremities is proportional to the number of eliminated spherical harmonics, and notably these extreme points are distributed along the boundary or perimeter of the magnet domain.

The next step is to establish and refine the superconducting coil geometries to optimize the magnetic field homogeneity within the inner field, while satisfying constraints such as the superconductor peak magnetic field condition and the fringe magnetic field strength.

The coil structures are initially positioned coincident with the positive maxima and negative minima current density contours with their initial cross sectional areas being proportional to the value of the associated current densities. The process of identifying and locating initial coils from the current density map is outlined in detail through illustrations in the results section. Using the seed coil layout obtained from the MSE current density map, the coil geometries are refined through a non-linear optimization method that minimizes the cost function F in a similar manner to that previously described for the MSE current density map calculation [12]:

$$\begin{aligned}\min_{I,L_k(y_{k,1},y_{k,2},z_{k,1},z_{k,2})} F_{\text{refine}} &= \frac{I^2}{2}\sum_{k=0}^{K-1} A_k^2 L_k, \\ &= \frac{I^2}{2}\sum_{k=0}^{K-1} \frac{31.6 y_{k,2}^2 (y_{k,1}-y_{k,2})^2 (z_{k,1}-z_{k,2})^2}{6y_{k,2}+9(z_{k,1}-z_{k,2})+10(y_{k,1}-y_{k,2})} 10^{-6},\end{aligned} \tag{1}$$

subject to:

$$\begin{aligned} &I\sum_{k=0}^{K-1}\alpha_{k,1} = B_0, \\ &I\sum_{n=1}^{N-1}\sum_{k=0}^{K-1}\alpha_{k,n} = 0, \\ &I\sum_{m=0}^{M-1}\sum_{k=0}^{K-1}\beta_{k,m} = 0, \\ &0 < I \leqslant I_{\max}, \end{aligned} \tag{2}$$

where, K is the number of the superconducting coils in the magnet domain and $(y_{k,1}, z_{k,1})$ and $(y_{k,2}, z_{k,2})$ are the coordinates of coil k with rectangular cross-section in the yz-plane, as shown in Fig. 1. For magnet configurations in which coils are coaxial and symmetric about the illustrated xy-plane, the spherical harmonic expansion results in the elimination of all even order terms within the expansion. To further reduce computational complexity, the strategy

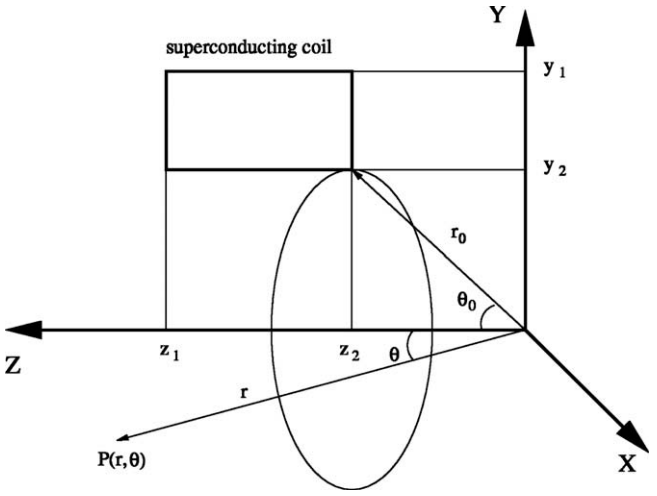

Fig. 1. Definition of the magnetic field at point $P(r, \theta)$ produced by a superconducting coil located in the yz-plane.

employed here considers only one quarter of the magnet domain, and thus, constraint (2) is simplified to:

$$\begin{aligned} &I\sum_{k=0}^{K-1}\alpha_{k,1} = \frac{B_0}{2}, \\ &I\sum_{n=1}^{N/2-1}\sum_{k=0}^{K-1}\alpha_{k,2n+1} = 0, \\ &I\sum_{m=0}^{M/2-1}\sum_{k=0}^{K-1}\beta_{k,2m+1} = 0, \\ &0 < I \leqslant I_{\max}, \end{aligned} \tag{3}$$

where K is the number of superconducting coils in one quarter of the magnet domain. It should be noted that within the optimization process the current densities are positive and are the same for all elements, and hence this applies to the coils as well. The sign of the current in a particular coil is implied by the order of the y_1 and y_2 coordinates. If $y_1 > y_2$, then the current has a positive sign, otherwise it has a negative sign. The need for negative currents and a more complicated optimization strategy within the computations is eliminated by using this approach.

Linear constraints were used for the determination of the MSE current density map, whereas in the refinement of the individual superconducting coils a constrained non-linear optimization problem is stated, requiring the use of an appropriate non-linear optimization algorithm to obtain the coil layout. One of the most effective methods of obtaining solutions to nonlinearly constrained optimization problems is to generate and solve quadratic subproblems. For this reason, sequential quadratic programming (SQP) [13]) is implemented to solve (1) subject to (2), (3). The SQP method is a local optimization algorithm, which yields globally optimal solutions given suitable initial starting values.

Through the optimization process the individual coil dimensions and spatial locations are altered, since L_k is a function of coil geometry, allowing the method to converge on a better minimized solution. Within the iterations the coils may overlap and so to avoid such situations, the magnet domain is divided into several layers and extra geometrical constraints based on the current density map are introduced to limit the movement of the coils. This step is fundamentally correct, since the current density maps do not suggest that the coils should be overlapped. In particular, limits on the y-coordinate of the individual coils are imposed by breaking the domain into layers to limit possible coil overlaps in this direction, and large axial movements are restricted by imposing z-coor-

dinate bounds. The values for $a_{l,p}$ and $b_{l,p}$ at position p and layer l must be non-negative, and in any given layer the sum of them must not be larger than the half length of the domain.

Fig. 2 is an illustration of a particular domain subdivision limiting coil overlap. As previously indicated, the current density extremities are distributed around the domain boundary, hence, the upper and lower domain subdivisions can have multiple coils and any sub-domain between them consists of a single coil.

After convergence has been achieved, the magnetic field experienced by the superconducting coils is calculated using the method outlined by Forbes et al [14]. If within the coils the peak field is greater than the allowable limit, then the individual layers are adjusted, to allow an increase in the spacing between problematic adjacent coils. For example, in Fig. 2 for the depicted three domain subdivision configuration, Y_1 and Y_2 are changed such that $|Y_2 - Y_1|$ is increased. The optimization process is then repeated to obtain the new coil layouts according to the new layer constraints. This process of iterative coil refinement may need to be repeated two or three times to ensure the optimum coil layout result.

3. Results and discussion

A number of design case studies have been conducted to illustrate the capability of the proposed superconducting magnet design approach. In this section, symmetric short bore magnet designs are provided for the shielded and unshielded cases.

In the following cases, the domain is limited in length to 1 m with inner bore diameter of 1 m, classifying the designs as short MRI magnets. The superconducting wires used in the designs are taken from Van Sciver and Marken [15]. All of the coils are formed using the least expensive 1×1 mm NbTi wires, by limiting the current density to a level below 180 A/mm and the peak magnetic field on the superconducting coils to be less than 9 T. It should be noted that the choice of NbTi wire represents the most difficult case given this superconductor's relatively low current carrying capacity and low critical peak field. Using Nb_3Sn alloy would allow design of magnets capable of higher field strengths.

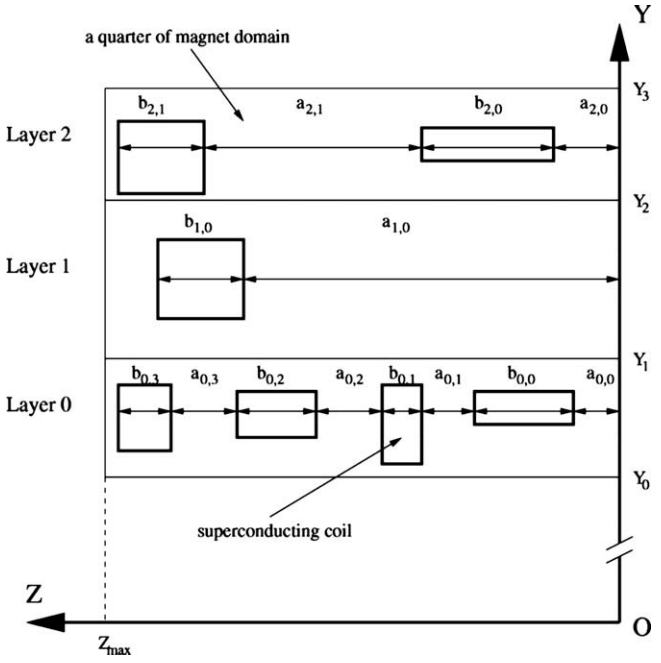

Fig. 2. An example superconducting coil layout and domain subdivision during the optimization stage.

3.1. Short bore unshielded magnets

An illustration of the order 16 degree 0 current density map is provided in Fig. 3(a) and the corresponding coil layout is given in Fig. 3(b), when no shielding requirements were given in the initial layout stage. Fig. 3(b) illustrates the numbering of the coils for the refinement stage. The distribution of the individual coils aligns with the current density map peaks, and the size of the coils is proportional to the magnitude of the current density at that location. In this manner, the initialised coils are reflective of the results obtained in Part I [12] for the MSE current density map. The coil refinement of (1) subject to (3) is then seeded using the coil distribution of Fig. 3(b) and rapid convergence is achieved, due to the fact that the initial seed is highly accurate.

Fig. 4(a) is an illustration of the final magnetic field and the associated DSV. For this magnet design the DSV is 50 cm in diameter to the 1 ppm contour line, and approximately 56 cm in diameter to the 10 ppm contour line. The footprint of this unshielded magnet is relatively large, as can be seen in Fig. 4(b).

The final coil configuration of Fig. 4(a) and corresponding coil numbering of Fig. 3(b) are given in Table 1. In the table, the (y_c, z_c) center coordinate of the individual coils is provided, with the number of superconducting wire windings defined as (N_y, N_z) in the radial and axial directions, respectively. The current density in the coils is 159 A/mm^2 and the maximum peak magnetic field on the superconducting coil was calculated to be 7.0741 T, which is well below the NbTi critical limit of 9.5 T at this current value [15].

As was highlighted earlier, the final configuration for the unshielded case has an alternating current direction coil layout around the perimeter of the magnet domain. It should also be noted that the largest coil is actually not on the inner layer of the magnet, but rather on the outer layer. At the manufacturing stage this may cause a radial stress related problem or a difficulty in quench protection, because of a possible inductance imbalance between coils. An increase in magnet domain length would see the external layer disappear, and the upper coil would be inline with the other lower coils. Since both cases have the same order, their DSV dimensions are the same. However, for shorter magnets the upper coils are introduced into the layout.

3.2. Short bore shielded magnet

For the case of a shielded magnet design the external magnetic field harmonic coefficients are used to reduce the stray field, which means that the number of coils has to be increased to allow for appropriate magnetic field definition. In optimization of the MSE current density map, nine harmonics (order 14 degree 4) were found to be appropriate for the design to obtain the current density map shown in Fig. 5(a). The corresponding coil configuration for refinement is illustrated in Fig. 5(b), whereby the coils themselves are allocated on the perimeter of the magnet domain, and the size of the coils is proportional to the current density for that particular extreme current density. Independent of the design strategy, that is whether unshielded or shielded, the current within the coils alternates as highlighted earlier.

Table 2 provides the dimensions and locations of the final coil layout. The current density in the wire is 159 A/mm^2 and the maximum peak field was calculated to be 8.9886 T, which is below the NbTi wire limit of 9.5 T at this current density value [15].

Fig. 6(a) is an illustration of the final optimized coil layout. It indicates that the DSV has a 40 cm diameter to the 1 ppm contour line and a diameter of 50 cm to the 10 ppm contour line. An important observation in this design is that the most outer coils do not necessarily have to be opposing current coils to limit the stray field of the magnet, but rather, these coils are used in conjunction with

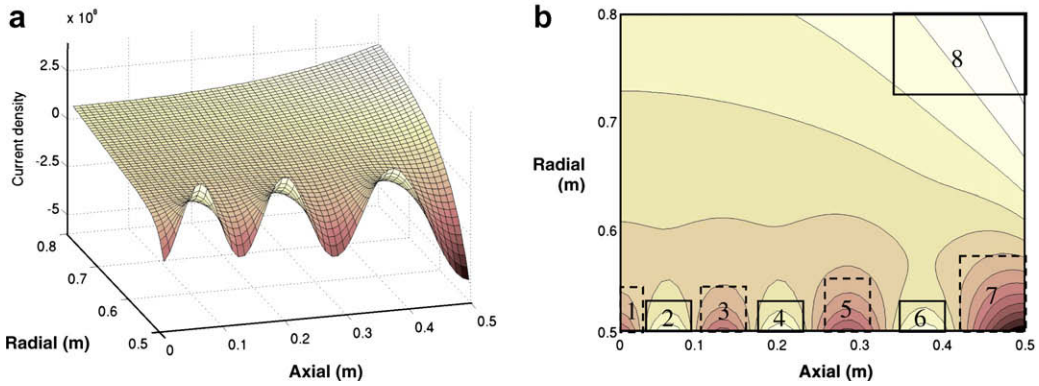

Fig. 3. The unshielded order 16 degree 0 magnet MSE current density profile in (a) 3D and (b) 2D with coil assignment for the layout refinement phase.

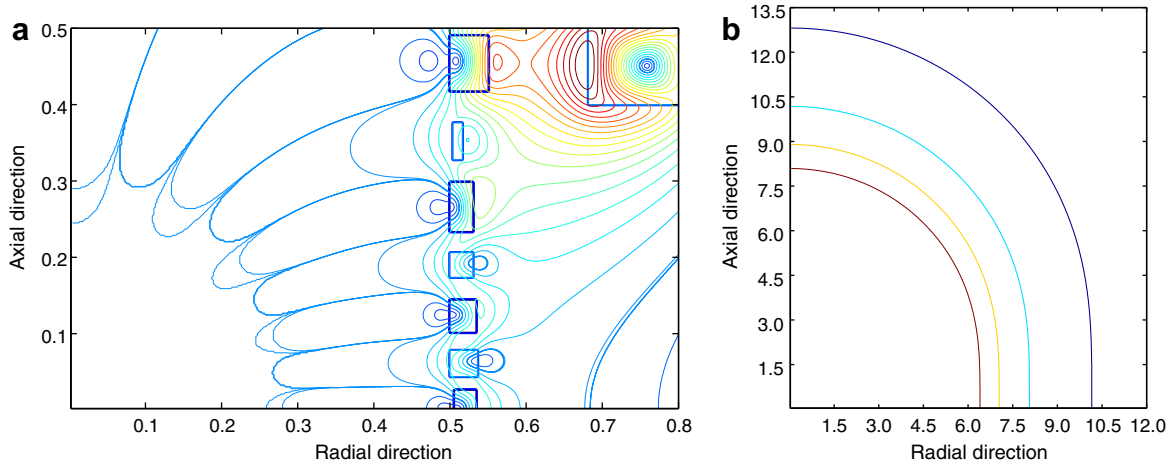

Fig. 4. The final configuration for the unshielded case. Illustrated are (a) the coil layout and associated magnetic field distribution, where the most inner contour corresponds to 1 ppm, followed by the 10 ppm contour and (b) the stray field with 5, 10, 15 and 20 G contour lines.

Table 1
Final coil allocation and dimensions for the unshielded configuration

Coil	I (A/mm^2)	y_c (m)	N_y	z_c (m)	N_z
1	−159	0.520532	29	0.012659	25
2	159	0.517828	36	0.061317	34
3	−159	0.516825	34	0.122282	42
4	159	0.515187	30	0.190080	33
5	−159	0.515190	30	0.265388	64
6	159	0.510032	12	0.352083	48
7	−159	0.525500	51	0.454366	71
8	159	0.740900	118	0.449593	101

the rest of other coils to obtain an overall effect satisfying both DSV and stray field requirements. The stray field for this design is depicted in Fig. 6(b), where the 5 G contour line extends no more than 4 m from the centre of the magnet.

4. Conclusion

A method of designing globally optimal magnets, and in particular MRI superconducting magnets but also applicable to other superconducting magnets such as those used in particle accelera-

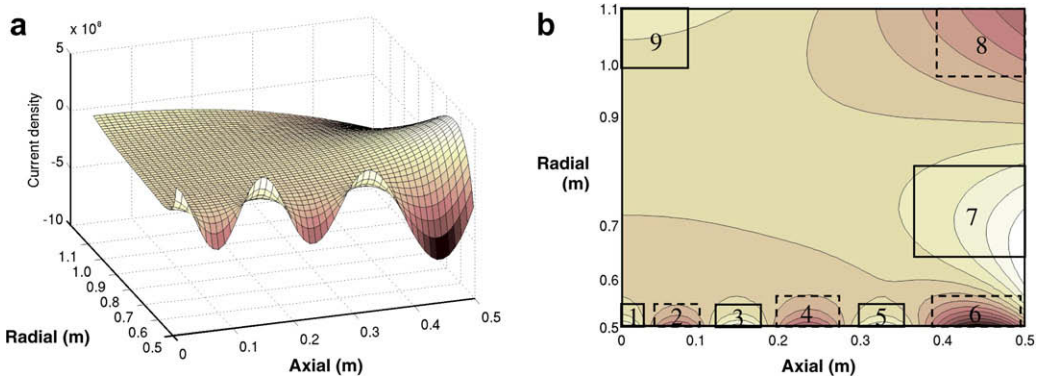

Fig. 5. The shielded order 14 degree 4 magnet MSE current density map in (a) 3D and (b) 2D with coil allocation for the location refining optimization phase.

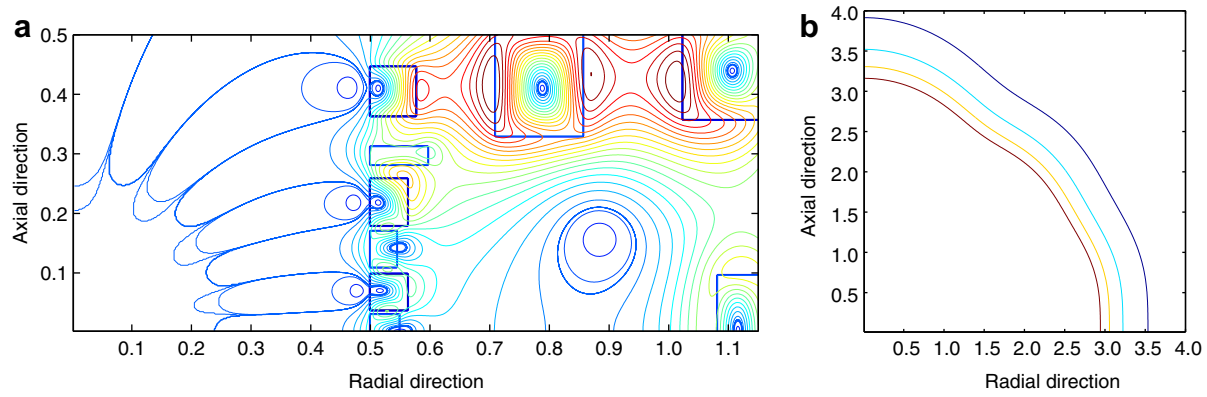

Fig. 6. The final configuration for the shielded case. Illustrated are (a) the coil layout and associated magnetic field distribution, where the most inner contour corresponds to 1 ppm, followed by the 10 ppm contour, and (b) the stray field with 5, 10, 15 and 20 G contour lines. This design has a smaller DSV and stray field due to the smaller order and larger degree, when compared to the design of Fig. 4.

Table 2
Final coil allocation and dimensions for the shielded configuration

Coil	I (A/mm^2)	y_c (m)	N_y	z_c (m)	N_z
1	159	0.523795	48	0.014565	29
2	−159	0.530974	62	0.068407	61
3	159	0.522495	45	0.139960	59
4	−159	0.531429	63	0.218645	79
5	159	0.548071	96	0.297088	29
6	−159	0.537711	75	0.405162	83
7	159	0.783175	146	0.414818	170
8	−159	1.087050	126	0.428726	143
9	159	1.115790	68	0.048344	97

tors, was outlined in detail. It was shown that a new two step optimization approach can be used to obtain high quality designs that allocate the magnet coils around the perimeter of the magnet domain. It was also shown that in compact designs the current in the coils should alternate between adjacent coils, to ensure that the required DSV and stray field constraints are met.

An unshielded and shielded design was illustrated for the case of short bore MRI superconducting magnets. Both designs yield magnet configurations that distribute coils around the perimeter of the magnet domain, whereby for the unshielded case different order and zero degree implementations can be used, and the degree is varied to meet the shielding design criteria. A key observation resulting from this approach is that irrespective of the shielding requirements, the coils themselves are located on the boundaries of the current density map domain, with the current direction alternating between adjacent coils.

The shielded magnet design produces a relatively well-confined stray field while allowing a relatively large DSV, given the overall magnet dimensions. The results described here are for spherical DSV magnets and the target region is defined accordingly. The work will be extended to allow for a more flexible definition of the DSV through target magnetic field values, essentially allowing for the formation of a non-spherical DSV. Furthermore, irregular superconducting coil shapes, as opposed to the regular rectangular cross-section coils will be considered, to allow for finer precision of the DSV.

In the design, the proposed method had included the field homogeneity in the DSV, the size of the stray field, critical current and peak field on the superconductor. However, it may be that in terms of manufacturing other constraints need to be placed on the magnet domain, to ensure adequate cryogenics, inter coil inductances leading to stresses and associated issues.

References

[1] G. Morrow, Progress in MRI magnets, IEEE Transactions on Applied Superconductivity 10 (2000) 744–751.
[2] H. Zhao, S. Crozier, A design method for superconducting MRI magnets with ferromagnetic material, Measurement Science and Technology 13 (2002) 2047–2052.
[3] H. Zhao, S. Crozier, Rapid field calculations for the effect of ferromagnetic material in MRI magnet design, Measurement Science and Technology 13 (2002) 198–205.
[4] V. Cavaliere, A. Formisano, R. Martone, M. Primizia, A genetic algorithm approach to the design of split coil magnets for MRI, IEEE Transactions on Applied Superconductivity 10 (2000) 1376–1379.
[5] J. Caldwell, Magnetostatic field calculations associated with superconducting coils in the presence of magnetic material, IEEE Transactions on Magnetics 18 (1982) 397–400.
[6] A.K. Kalafala, Optimized configurations for actively shielded magnetic resonance imaging magnets, IEEE Transactions on Magnetics 27 (1991) 1696–1699.
[7] A. Zisserman, R. Saunders, J. Caldwell, Analytic solutions for axisymmetric magnetostatic systems involving iron, IEEE Transactions on Magnetics 23 (1987) 3895–3902.
[8] A. Ishiyama, M. Hondoh, N. Ishida, T. Onuki, Optimal design of MRI magnets with magnetic shielding, IEEE Transactions on Magnetics 25 (1989) 1885–1888.
[9] A. Ishiyama, H. Hirooka, Magnetic shielding for MRI superconducting magnets, IEEE Transactions on Magnetics 27 (1991) 1692–1695.
[10] A.K. Kalafala, A design approach for actively shielded magnetic resonance imaging magnets, IEEE Transactions on Magnetics 26 (1990) 1181–1188.
[11] B. Zhang, C. Gazdzinski, B.A. Chronik, H. Xu, S.M. Conolly, B.K. Rutt, Simple design guidelines for short MRI systems, Concepts in Magnetic Resonance Part B 25B (2005) 53–59.
[12] Q.M. Tieng, V. Vegh, I.M. Brereton, Globally Optimal Superconducting Magnets Part I: Minimum Stored Energy (MSE) Current Density Map, Journal of Magnetic Resonance 196 (2009) 1–6.
[13] C. Lawrence, J.L. Zhou, A.L. Tits, User's Guide for CFSQP Version 2.5: A C Code for Solving (Large Scale) Constrained Nonlinear (Minimax) Optimization Problems, Generating Iterates Satisfying All Inequality Constraints, University of Maryland, 1997.
[14] L.K. Forbes, S. Crozier, D.M. Doddrell, Rapid computation of static fields produced by thick circular solenoids, IEEE Transactions on Magnetics 33 (1997) 4405–4410.
[15] S.W.V. Sciver, K.R. Marken, Superconducting magnets above 20 T, Physics Today (2002) 37–42.